Optics Letters

Absolute frequency measurements of CHF_3 Doppler-free ro-vibrational transitions at 8.6 μm

Alessio Gambetta,[1,2] Edoardo Vicentini,[1] Yuchen Wang,[1] Nicola Coluccelli,[1,2] Eugenio Fasci,[3] Livio Gianfrani,[3] Antonio Castrillo,[3] Valentina Di Sarno,[4] Luigi Santamaria,[5] Pasquale Maddaloni,[4,6] Paolo De Natale,[4] Paolo Laporta,[1,2] and Gianluca Galzerano[1,2,*]

[1]Dipartimento di Fisica—Politecnico di Milano, Piazza Leonardo da Vinci 32, 20133 Milano, Italy
[2]Istituto di Fotonica e Nanotecnologie—CNR, Piazza Leonardo da Vinci 32, 20133 Milano, Italy
[3]Dipartimento di Matematica e Fisica—Università degli studi della Campania "Luigi Vanvitelli," Viale Lincoln 5, 81100 Caserta, Italy
[4]CNR-INO, Istituto Nazionale di Ottica, Via Campi Flegrei 34, 80078 Pozzuoli (NA), Italy
[5]Agenzia Spaziale Italiana—Centro di Geodesia Spaziale, Matera 75100, Italy
[6]INFN, Istituto Nazionale di Fisica Nucleare, Sez. di Napoli, Complesso Universitario di M.S. Angelo, Via Cintia, 80126 Napoli, Italy
*Corresponding author: gianluca.galzerano@polimi.it

Received 27 February 2017; revised 12 April 2017; accepted 12 April 2017; posted 13 April 2017 (Doc. ID 287557); published 5 May 2017

We report on absolute measurements of saturated-absorption line-center frequencies of room-temperature trifluoromethane using a quantum cascade laser at 8.6 μm and the frequency modulation spectroscopy method. Absolute calibration of the laser frequency is obtained by direct comparison with a mid-infrared optical frequency comb synthesizer referenced to a radio-frequency Rb standard. Several sub-Doppler transitions falling in the υ_5 vibrational band are investigated at around 1158.9 cm^{-1} with a fractional frequency precision of $8.6 \cdot 10^{-12}$ at 1-s integration time, limited by the Rb-clock stability. The demonstrated frequency uncertainty of $6.6 \cdot 10^{-11}$ is mainly limited by the reproducibility of the frequency measurements.

OCIS codes: (140.5965) Semiconductor lasers, quantum cascade; (140.3425) Laser stabilization; (140.7090) Ultrafast lasers; (300.6320) Spectroscopy, high-resolution.

https://doi.org/10.1364/OL.42.001911

Trifluoromethane, CHF_3, is one of the protagonists in the emerging field of cold stable molecules with very promising new insights into fundamental physics, as well as into applications ranging from quantum simulations to controlled chemistry [1,2]. Therefore, the availability of novel, high-precision spectroscopic data for this molecule is of utmost relevance, particularly in the mid-infrared (MIR) spectral window, where most of the fundamental-band ro-vibrational transitions fall. So far, however, the vast majority of spectroscopic measurements have been carried out by Fourier-transform-infrared (FTIR) spectroscopy [3–7], with a spectral resolution that has not exceeded 0.004 cm^{-1} (120 MHz), obtained in the 8–9 μm interval (υ_2 and υ_5 fundamental bands) with a CHF_3 free-jet expansion [8–10]. Superior frequency resolutions have been occasionally achieved using laser absorption spectroscopy; in one case, several ro-vibrational lines in the υ_4 fundamental band were measured from 1361 to 1385 cm^{-1} with a resolution of 30 MHz by a tunable lead-salt diode laser [11,12]. In a previous work, by exploiting a quantum cascade laser (QCL) frequency locked to an optical frequency comb synthesizer (OFCS), we recorded several ro-vibrational transitions belonging to the υ_5 band at 8.6 μm, demonstrating a resolution of 20 kHz in the line-center frequency determination [13]. To further improve the measurement accuracy, implementation of a sub-Doppler spectroscopic technique is needed. Up to now, restricted by technical hurdles, sub-Doppler spectroscopy of trifluoromethane has been reported only in a couple of works. In the former case, bolometric detection performed by a color-center laser on a cold (4 K) CHF_3 beam was used to observe saturation resonances in the υ_1 fundamental band (around 3035 cm^{-1}) with a full width at half-maximum (FWHM) of 10 MHz [14]. In the latter experiment, sub-Doppler absorption features with a FWHM as low as 200 kHz were recorded by CO_2 laser-sideband spectroscopy in the CDF_3 υ_5 fundamental band [15].

In this Letter, based on an OFCS-referenced QCL emitting at 8.6 μm, Doppler-free frequency modulation (FM) saturated absorption spectroscopy is demonstrated on several ro-vibrational components of the CHF_3 υ_5 band. In particular, absolute measurements of the Lamb-dip center frequencies are reported with a precision as low as 300 Hz (8.6×10^{-12} in factional terms) at 1-s integration time, essentially limited by the stability of the adopted reference (GPS-disciplined Rb clock). A comprehensive characterization of the main contributions to the measurement uncertainty is also presented, leading to a combined uncertainty in the determination of the sub-Doppler line-center frequencies of 2 kHz (6.6×10^{-11}), basically ascribable to the reproducibility of the implemented frequency measurement (FM) spectroscopic setup.

The experimental setup for Doppler-free FM saturated absorption spectroscopy of CHF_3 is shown in Fig. 1. The probe laser source is a continuous-wave (CW) distributed-feedback

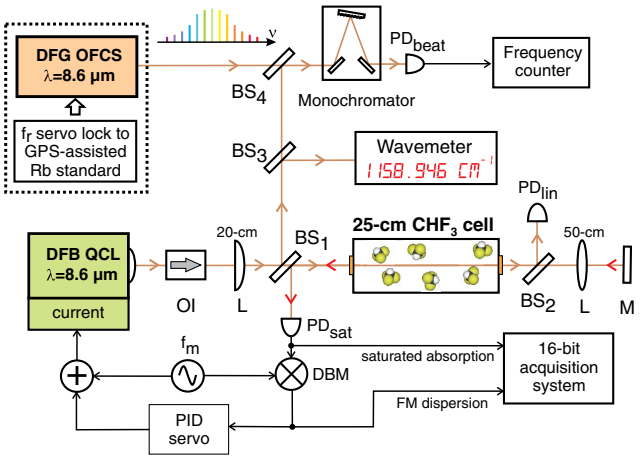

Fig. 1. Experimental setup for Doppler-free FM spectroscopy of CHF_3 at 8.6 μm. BS, beam splitter; DBM, doubled-balanced mixer; DFG OFCS, difference-frequency-generation optical frequency comb synthesizer; L, lens; M, mirror; OI, optical isolator; PID, proportional-integrative-derivative servo.

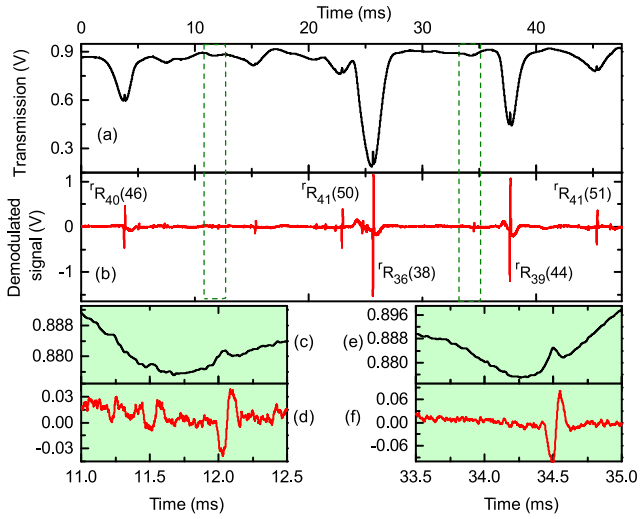

Fig. 2. (a) Saturated absorption and (b) FM dispersive signal from a 25-cm-long cell filled a with CHF_3 gas sample at 10 Pa ($f_m = 1.5$ MHz, $a_m = 1.5$ MHz, 100-kHz demodulation bandwidth). (c)–(f) Expanded view of selected portions in the recorded profiles, showing that even for a congested spectrum (like that of room-temperature CHF_3 at 8.6 μm), the implemented FM saturated absorption scheme is able to dramatically increase the accuracy of the spectral analysis compared to the linear absorption regime.

(DFB) QCL with a maximum output power of ~40 mW, tunable in the wavelength range from 8.55 to 8.65 μm. Its current driver, with a noise spectral-density as low as $3\text{nA}/\sqrt{\text{Hz}}$, has an electrical modulation bandwidth of 2 MHz. Active control of the QCL temperature with a stability of a few mK over more than 1 h is accomplished via a Peltier cooler driven by a commercial temperature controller. Fine tunability in the frequency range from 1158 to 1161 cm^{-1} is fulfilled by a proper combination of laser current ($\Delta\nu/\Delta I = -0.011$ cm^{-1}/mA) and temperature ($\Delta\nu/\Delta T = -0.086$ $\text{cm}^{-1}\,\text{K}^{-1}$) adjustments. After emerging from a 30 dB optical isolator, the QCL output beam is collimated by a ZnSe plano-convex lens (20-cm focal length) followed by a 50% beam splitter (BS1) whose transmission propagates as the strong pump beam through a 25-cm-long stainless-steel cell (equipped with antireflection coated ZnSe windows) containing the CHF_3 gas sample (98% purity) at room temperature, T_{room}, with a measured beam waist diameter of 2.1 mm in the middle of the absorption cell. Reflection from a second 50% beam splitter (BS2) is directed to a liquid-nitrogen-cooled HgCdTe (MCT) detector (1-MHz electrical bandwidth), PD_{lin}, to record the single-pass absorption; transmission from BS2 passes through a 50-cm focusing lens and it is back-reflected by a mirror to generate the counter-propagating weak probe beam (1/4 of the pump beam power), which is then superimposed to the pump beam in the gas cell with matched phase fronts (probe beam waist diameter of 1.8 mm). Eventually, to detect the saturated absorption signal, the probe beam is reflected by BS1 onto a four-stage thermoelectrically cooled MCT detector (50 MHz bandwidth), PD_{sat}; with this scheme, a pump beam intensity of $\simeq 190$ mW/cm^2 and a CHF_3 pressure of 10 Pa (75 mTorr) are typically used to acquire the Lamb-dip signals. For this intensity, we did not observe any contribution from probe-self pumping [16], although the pump-to-probe ratio was changed in the range from 2:1 to 8:1.

To implement the FM technique [17,18], the QCL driving current is modulated at a frequency $f_m = 1.56$ MHz with a modulation depth $a_m = 1.5$ MHz (corresponding to a nearly unitary phase modulation index). Figure 2 shows both (a) the saturated absorption and (b) the FM dispersion profile (in-phase first-harmonic demodulated signal) recorded by scanning, via the driving current, the QCL frequency by ~2 GHz around 1158.9 cm^{-1}. From panel (a), a detection sensitivity $\alpha_{\text{min}} = 2 \cdot 10^{-5}$ cm^{-1} (1 MHz integration bandwidth) is estimated, mainly limited by the QCL intensity noise for Fourier frequencies lower than 100 kHz, and by the detector noise for Fourier frequencies in the range from 0.1 to 10 MHz. From panel (b), it can be appreciated that a further improvement down to $\alpha_{\text{min}} = 5 \cdot 10^{-7}$ cm^{-1} (100-kHz integration bandwidth), with an effective suppression of spurious etalon effects, is brought about by the FM spectroscopy approach. In particular, for the most intense saturated line, a signal-to-noise ratio (SNR) larger than 250 (48 dB) is achieved. Thanks to this sensitivity, several tens of saturated absorption lines could be detected, with Lamb-dip linewidths (FWHM) and contrasts ranging from 1.5 to 2 MHz and from 5% to 30% (with respect to the linear absorption contrast), respectively. In particular, the measured Lamb-dip linewidths are substantially determined by pressure and power broadening effects, with the transit-time broadening contribution and the QCL emission linewidth being at a level of 100 kHz and 600 kHz, respectively. The difference in the measured Lamb-dip linewidths is therefore due to the different values of pressure-broadening coefficients and saturation intensities of the investigated transitions [13].

In order to measure the absolute line-center frequency of a given CHF_3 transition, the QCL frequency is first locked to the zero of the corresponding (dispersive) FM saturated absorption signal using a proportional-integrative-derivative (PID) servo controller acting on the QCL driving current. Then, the frequency-stabilized QCL is beaten against a suitable MIR OFCS covering the 8–14-μm spectral region [19]. Produced without any carrier-envelope offset via difference frequency

generation (DFG) in a GaSe nonlinear crystal, starting from a dual-branch 250-MHz Er:fiber laser oscillator, this optical comb is properly tuned to a central wavelength of 8.6 μm, with an average output power of 4 mW in an optical bandwidth of 0.8 μm (corresponding to 0.22 μW per comb tooth). The comb repetition rate, $f_r = 250$ MHz, is stabilized against a radio-frequency (RF) synthesizer locked, in turn, to a GPS-disciplined Rb clock; this latter frequency-reference chain has a fractional frequency stability (1-s Allan deviation) and accuracy of $8 \cdot 10^{-12}$ and 10^{-13}, respectively. The MIR OFCS and the QCL beams are then superimposed using a 50% ZnSe beam-splitter (BS4); after filtering by means of a 0.01-μm monochromator, the combined beams are focused onto a 200-MHz bandwidth MCT detector, PD_{beat}, ($5.7 \cdot 10^4$ V/W responsivity and 50 nV/$\sqrt{\text{Hz}}$ noise floor at a temperature of 77 K). Figure 3(a) shows the RF spectrum of the photocurrent measured when the QCL is operated in free-running mode. Three main peaks are clearly distinguished from the background noise: the beat-note signal at $f_{beat} \simeq 53$ MHz between the QCL mode and the nearest comb tooth, the comb repetition rate at 250 MHz, and the beat note between the QCL mode and the second-nearest comb tooth (at a frequency of ≃197 MHz). The main beat note, observed with a SNR of 40 dB, is characterized by a FWHM linewidth of 600 kHz for an integration time of 50 μs [blue curve in Fig. 3(b)]. Further linewidth narrowing of the beat note, down to 100 kHz, is obtained when the QCL is frequency stabilized, as an example, against the FM saturated absorption signal of the $^rR_{38}(36)$ ro-vibrational component [red curve in Fig. 3(b)]. The 100-kHz QCL line narrowing is mainly limited by the 350-kHz control-loop bandwidth, which turns out to be strictly linked to the FM demodulation electronics' finite bandwidth of 100 kHz. In this configuration, the absolute frequency of the stabilized QCL is determined through the relation $\nu_{QCL} = nf_r \pm f_{beat}$, where n is the comb mode order, unambiguously determined by a 50-MHz-accuracy wavemeter (the ±1 factor uncertainty is removed by measuring the sign in the beat-note frequency change with respect to a slight variation in the comb repetition rate).

To characterize the frequency stability of the Lamb-dip-locked QCL, the main beat-note frequency was directly measured by a reciprocal electronic counter without any additional

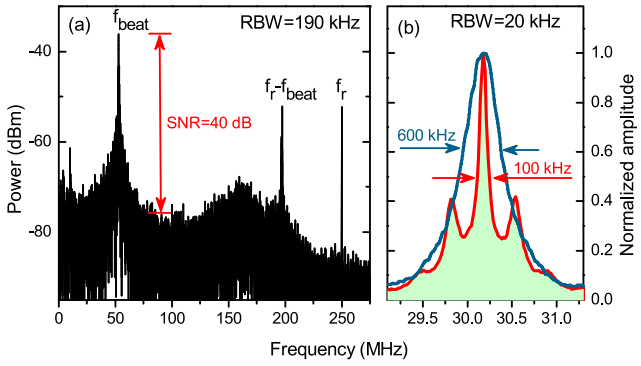

Fig. 3. RF spectrum of the beat signal between the MIR OFCS and the QCL: (a) QCL in free-running operation (frequency span from DC to 260 MHz, 190-kHz resolution bandwidth); (b) QCL frequency stabilized against the FM saturated absorption of the $^rR_{36}(38)$ line; as inferred by the spectral position of the servo bumps, here the closed-loop bandwidth is ~350 kHz.

phase-locked loop (transfer oscillator method). Figure 4(a) shows the corresponding Allan deviation (open circles) versus the integration time, τ, when the QCL is locked against the $^rR_{36}(38)$ line for a CHF_3 pressure of 7 Pa (corresponding to the maximum SNR). In the same diagram, the Allan deviation of the Rb clock (black curve), measured against a hydrogen maser, is also reported for comparison. The QCL Allan deviation reaches a minimum value of 8.6×10^{-12} at $\tau = 1$ s, which turns out to be limited by the frequency stability of the adopted Rb clock. For shorter integration times, the stability is characterized by a white phase noise contribution, $\sigma(\tau) = 10^{-12} \cdot \tau^{-1}$, indicating a tight phase-locking between the QCL and the Lamb-dip reference. For $\tau > 1$ s, a linear drift of 4.5 kHz/min limits the long-term stability of the frequency stabilized QCL; this drift, essentially due to the air-pressure-induced shift caused by the relatively high leakage (0.14 Pa/min) from the gas cell, prevented us from extending the duration of these measurement sets far above 100 s. By removing from the data the measured linear frequency drift, the Allan deviation is limited at the level of $8 \cdot 10^{-12}$ by a flicker frequency noise contribution.

Afterwards, to thoroughly investigate any systematic effects in the line-center frequency determinations, we also measured the sensitivity coefficient of the Lamb-dip-locked QCL frequency against the CHF_3 pressure and gas cell leakage, the pump and probe beam powers, the modulation frequency and depth, the electronic offsets, and the etalon effects. Just as an example, Fig. 4(b) shows the measured $^rR_{36}(38)$ line-center frequency for different CHF_3 pressures, yielding a pressure-shift coefficient of (22 ± 1) kHz/Pa. The other sensitivity coefficients, together with their influence on the systematic (type B) uncertainty of the absolute line-center frequency measurement, are listed in Table 1. Such an analysis reveals that the major sources of type B uncertainties are due to the 0.5% accuracy of the absolute pressure gauge used in the experiments and the measured pressure shift

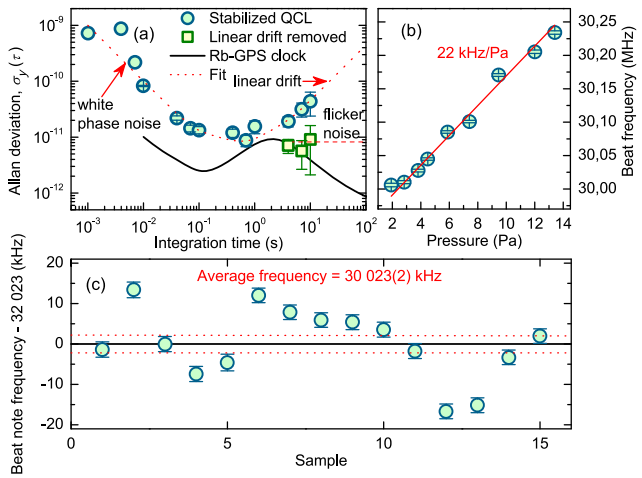

Fig. 4. Absolute frequency measurements. (a) Allan deviation of the Lamb-dip-locked QCL frequency versus the integration time. The dotted red line represents the best interpolation curve, $\sigma_y^2(\tau) = 10^{-24}/\tau^2 + 0.6 \cdot 10^{-22} + 6 \cdot 10^{-24}\tau^2$. (b) Pressure-shift measurement of the $^rR_{36}(38)$ line. (c) Reproducibility in the line-center frequency determination for different measurement sets, carried out under the same experimental conditions. The error bars represent the combined (type A and B) uncertainty, whereas the dotted red line is the rms of the average value.

Table 1. Measured Sensitivity Coefficients for the $^rR_{36}(38)$ Line and Their Contribution to the Uncertainty Budget

Parameter	Coefficient	Type B Uncertainty (kHz)
CHF_3 pressure, p_{CHF_3}	22(1) kHz/Pa	0.75
Gas cell leakage, p_{leak}	38(2) kHz/Pa	1.5
Laser power, P_{QCL}	45 kHz/mW	0.2
Modulation frequency, f_m	100 Hz/kHz	Negligible
Modulation depth, a_m	16 kHz/MHz	Negligible
Electronic offset	0.3 kHz/mV	0.2
Etalon/interference effects		0.5
Rb-GPS clock		0.04
Total type B uncertainty		1.8 ($5 \cdot 10^{-11}$)

coefficient (corresponding to 0.75 kHz), and to the gas cell leakage during the measurement time (1.5 kHz). Taking into account all the contributions, the estimated total type B uncertainty is 1.8 kHz, corresponding to a fractional accuracy of $5 \cdot 10^{-11}$.

Finally, to check the reproducibility of the line-center frequency determination, for fixed experimental operating parameters ($p_{CHF_3} = 7.00 \pm 0.04$ Pa, $T_{room} = 22.1 \pm 0.5$C°, $P_{pump} = 5$ mW, $P_{probe} = 1.3$ mW, $f_m = 1.56$ MHz, $a_m = 1.5$ MHz), repeated measurements were performed with an integration time of 1 s (corresponding to the minimum Allan deviation) and a measurement time of 100 s. Figure 4(c) reports fifteen independent measurements as performed over a few days, returning a rms deviation of 2.3 kHz (6.6×10^{-11}), in a good agreement with the estimated type B uncertainty. The measured average frequency of the QCL stabilized is 34 743 125 035(2) kHz ($n = 138972$ and $f_r = 250001115.75$ Hz). Taking into account the pressure-shift coefficient, the line-center frequency of the $^rR_{36}(38)$ transition extrapolated at zero pressure is 34 743 124 881(2) kHz (1 158.905 901 53(8) cm^{-1}).

Our spectroscopic investigation was focused on the particular spectral region at around 1158.9 cm^{-1} in coincidence with the $^pR_1(1)$ line belonging to the υ_5 band ($J' = 2$, $K' = 0$, $l' = 1$, $J = 1$, $K = 1$, and $l = 0$) in view of a future test on the time constancy of the proton-to-electron mass ratio [20]. For this application, extension of such an investigation to the low-temperature regime (below 10 K) is planned with a buffer-gas-cooling source [21]. In conclusion, we report on the saturated-absorption spectroscopy of the CHF_3 υ_5 vibrational band by using a QCL at 8.6 μm and the FM spectroscopy method. Absolute measurements of the sub-Doppler line-center frequencies have been obtained by using a difference-frequency-generation mid-IR frequency comb, frequency stabilized with respect to a GPS-disciplined Rb frequency standard. The demonstrated fractional precision and accuracy of $8.6 \cdot 10^{-12}$ and $6.6 \cdot 10^{-11}$, respectively, were mainly limited by the stability and by the reproducibility of the developed FM spectrometer. Further improvements in the frequency measurements can be obtained using a 77-K hermetic gas cell operating at a pressure of 1 Pa or even lower. The method above proposed can be immediately extended to realize a compact and fully transportable molecular-gas-cell optical frequency standard in the mid-infrared with a potential accuracy at the 10^{-12} level.

Funding. Ministero dell'Istruzione, dell'Università e della Ricerca (MIUR) (RBFR1006TZ).

Acknowledgment. The authors acknowledge Dr. Adina Ceausu-Velcescu for the theoretical identification of the investigated CHF_3 transitions.

REFERENCES

1. C. Sommer, L. D. van Buuren, M. Motsch, S. Pohle, J. Bayerl, P. W. H. Pinkse, and G. Rempe, Faraday Discuss. **142**, 203 (2009).
2. S. Chervenkov, X. Wu, J. Bayerl, A. Rohlfes, T. Gantner, M. Zeppenfeld, and G. Rempe, Phys. Rev. Lett. **112**, 013001 (2014).
3. N. J. Fyke, P. Lockett, J. K. Thompson, and P. M. Wilt, J. Mol. Spectrosc. **58**, 87 (1975).
4. S. Kondo and S. Saëki, J. Chem. Phys. **74**, 6603 (1981).
5. J. P. Champion and G. Graner, Mol. Phys. **58**, 475 (1986).
6. R. McPheat and G. Duxbury, J. Quant. Spectrosc. Radiat. Transfer **66**, 153 (2000).
7. J. J. Harrison, J. Quant. Spectrosc. Radiat. Transfer **130**, 359 (2013).
8. H.-R. Dübal and M. Quack, J. Chem. Phys. **81**, 3779 (1984).
9. A. Amrein, M. Quack, and U. Schmitt, Mol. Phys. **60**, 237 (1987).
10. A. Amrein, M. Quack, and U. Schmitt, J. Phys. Chem. **92**, 5455 (1988).
11. S. Sofue, K. Kawaguchi, E. Hirota, and T. Fujiyama, Bull. Chem. Soc. Jpn. **54**(3), 897 (1981).
12. S. Sofue, K. Kawaguchi, E. Hirota, and T. Fujiyama, Bull. Chem. Soc. Jpn. **54**(11), 3546 (1981).
13. A. Gambetta, N. Coluccelli, M. Cassinerio, T. T. Fernandez, D. Gatti, A. Castrillo, A. Ceausu-Velcescu, E. Fasci, L. Gianfrani, L. Santamaria, V. Di Sarno, P. Maddaloni, P. De Natale, P. Laporta, and G. Galzerano, J. Chem. Phys. **143**, 234202 (2015).
14. A. S. Pine, G. T. Fraser, and J. M. Pliva, J. Chem. Phys. **89**, 2720 (1988).
15. P. Pracna, K. Sarka, J. Demaison, J. Cosleou, F. Herlemont, M. Khelkhal, H. Fichoux, D. Papousek, M. Paplewski, and H. Bürger, J. Mol. Spectrosc. **184**, 93 (1997).
16. B. E. Sherlock and I. G. Hughes, Am. J. Phys. **77**, 111 (2009).
17. G. C. Bjorklund, Opt. Lett. **5**, 15 (1980).
18. S. Borri, S. Bartalini, P. De Natale, M. Inguscio, C. Gmachl, F. Capasso, D. Sivco, and A. Cho, Appl. Phys. B **85**, 223 (2006).
19. A. Gambetta, N. Coluccelli, M. Cassinerio, D. Gatti, P. Laporta, G. Galzerano, and M. Marangoni, Opt. Lett. **38**, 1155 (2013).
20. L. Santamaria, V. Di Sarno, I. Ricciardi, S. Mosca, M. De Rosa, G. Santambrogio, P. Maddaloni, and P. De Natale, J. Mol. Spectrosc. **300**, 116 (2014).
21. S. E. Maxwell, N. Brahms, D. Glenn, J. Helton, S. Nguyen, D. Patterson, J. Petricka, D. DeMille, and J. Doyle, Phys. Rev. Lett. **95**, 173201 (2005).